Research Article | Vol. 30, No. 21 / 10 Oct 2022 / Optics Express 37910

Optics EXPRESS

Simple yet effective analysis of waveguide mode symmetry: generalized eigenvalue approach based on Maxwell's equations

WENFEI GUO,[1] YANTAO WU,[1] ZHONGFEI XIONG,[1] YUHAO JING,[1] AND YUNTIAN CHEN[1,2,3,*]

[1] School of Optical and Electronic Information, Huazhong University of Science and Technology, Wuhan 430074, China
[2] Wuhan National Laboratory of Optoelectronics, Huazhong University of Science and Technology, Wuhan 430074, China
[3] Optics Valley Laboratory, Hubei 430074, China
[*] yuntian@hust.edu.cn

Abstract: Particular waveguide structures and refractive index distribution can lead to specified degeneracy of eigenmodes. To obtain an accurate understanding of this phenomenon, we propose a simple yet effective approach, i.e., generalized eigenvalue approach based on Maxwell's equations, for the analysis of waveguide mode symmetry. In this method, Maxwell's equations are reformulated into generalized eigenvalue problems. The waveguide eigenmodes are completely determined by the generalized eigenvalue problem given by two matrices (M, N), where M is 6×6 waveguide Hamiltonian and N is a constant singular matrix. Close examination shows that N usually commute with the corresponding matrix of a certain symmetry operation, thus the waveguide eigenmode symmetry is essentially determined by M, in contrast to the tedious and complex procedure given in the previous work [Opt. Express **25**, 29822 (2017)]. Based on this new approach, we discuss several symmetry operations and the corresponding symmetries including chiral, parity-time reversal, rotation symmetry, wherein the constraints of symmetry requirements on material parameters are derived in a much simpler way. In several waveguides with balanced gain and loss, anisotropy, and geometrical symmetry, the analysis of waveguide mode symmetry based on our simple yet effective approach is consistent with previous results, and shows perfect agreement with full-wave simulations.

1. Introduction

Symmetries are admittedly significant in many subfields of physics [1]. In optics, symmetries impose constraints on electromagnetic responses and can be used to simplify complex optical structures [2–4]. In waveguide system, the degeneracy of eigenmodes is closely related to the symmetry of the structure. If the waveguide system contains a certain symmetry, one eigenmode can transform to its degenerated mode (or itself) under the specific symmetry operation corresponding to the symmetry. One example is the $\mathcal{PT}$ (parity-time reversal) operation and $\mathcal{PT}$ symmetry, which has been studied extensively [5–8]. Some astonishing behaviours of light can be realized in certain well-designed optical structures with $\mathcal{PT}$ symmetry [9,10]. In the parameter space, there exists exceptional points (EPs) at which the transition between $\mathcal{PT}$ symmetry unbroken phase and broken phase occurs [9,11], where the symmetry properties of those eigenmodes transforms differently. Moreover, one useful theoretical framework to handle such $\mathcal{PT}$ symmetric optical systems with gain and loss is the coupled mode theory (CMT). In CMT, the new eigenmodes under perturbation are expanded by forward and backward propagation modes [11,12]. Therefore, a close examination on the connection between forward

#472148 https://doi.org/10.1364/OE.472148
Journal © 2022 Received 4 Aug 2022; revised 11 Sep 2022; accepted 11 Sep 2022; published 28 Sep 2022

Optics EXPRESS

and backward propagation modes is beneficial for applying CMT to waveguides with gain and loss, anisotropy, and bianisotropy.

In addition, the polarization of modes in waveguides is also of interest. By manipulating the polarization of light, the optical angular momentum can be generated, which leads to some emerging applications in optical communication [13,14]. If the waveguide structure contains geometrical symmetry such as rotation or mirror reflection symmetry, degeneracy between eigenmodes with different polarization may occur. In this case, the two degenerated eigenmodes propagate in the same direction. Accounting for the vectorial nature of the electromagnetic field, the rotation and mirror reflection operator acting on the eigenmodes should be defined properly [15].

All the discrete symmetry operations of optical systems such as the dual symmetry between electric and magnetic fields, time reversal symmetry, and many more, can be essentially interpreted and mathematically proved from Maxwell's equations. However, the familiar differential and integral forms of Maxwell's equations are not intuitive enough to reveal the intrinsic symmetry properties of optical systems, especially for waveguide problems. Reformulating Maxwell's equations into an eigen equation with the waveguide Hamiltonian can yield straightforward classification and analysis of the mode symmetry without solving Maxwell's equations exactly. One approach proposed by Xiong *et al.* is to eliminate the longitudinal components of the field (i.e. e_z and h_z) and get a 4×4 waveguide Hamiltonian [16]. However, the Hamiltonian derived in this approach contains second order partial derivatives with respect to x and y, which makes the calculations extremely complicated in computing the commutation relation associated with Hamiltonian and symmetry operators. In addition, the absence of z field components in the wave function is also a barrier to intuitive analysis of the z components symmetry.

Here, we propose a simple yet effective approach to examine waveguide mode symmetry by including e_z and h_z components explicitly [16]. Firstly, the waveguide problem is reformulated into a generalized eigenvalue problem containing two matrices (M, N), where M is the 6×6 effective waveguide Hamiltonian and N is a constant singular matrix. The matrix form of Hamiltonian M contains only first order partial derivatives of x and y, which is easier and more transparent to study the mode symmetry with all six field components. By imposing the symmetry operators with proper 6×6 matrix, we analysis several common symmetries via the commutation relations between symmetry operators and waveguide Hamiltonian M in few concrete examples.

The paper is organized as follows. In Section 2, we illustrate the general approach to the construction of the generalized eigenvalue problem for waveguides, and discuss six common symmetries as well as the combinations of them. In Section 3, we analyze the symmetry properties of gain-loss balanced and anisotropic waveguides, as well as the mode properties between the forward and backward propagating waveguide modes under parity/chiral/time reversal symmetry. Finally, Section 4. summarizes the paper.

2. Theory

In this section, we develop a general procedure for analyzing the waveguide mode symmetry. The eigen equation for waveguide problems is derived, which is similar to the stationary Schrödinger equation. Assuming the waveguide has translational symmetry along the propagation direction (z axis), the eigenmode with a definite propagation constant β can be expressed as $\Phi(x, y, z) = \boldsymbol{\phi}(x, y)e^{-i\beta z}$, which resembles the stationary wave function $\Phi(\boldsymbol{r}, t) = \phi(\boldsymbol{r})e^{-iEt}$. The position variable z is corresponding to time t and the propagation constant β is corresponding to the energy E [17].

The material of the waveguide core can be active, passive, anisotropic or bianisotropic. The geometrical shape of the waveguide cross-section can be symmetric or irregular. Adapting Cartesian coordinate system, the cross-section of waveguide is in the xy plane and the propagation direction is along the z axis. The background material is assumed to be homogeneous and isotropic. Therefore, the symmetry property of waveguide modes is mainly determined by the waveguide core.

2.1. Hamiltonian formulation of waveguide problems

The constitutive relation in general bianisotropic waveguides is expressed as follows [12]:

$$\boldsymbol{D} = \bar{\boldsymbol{\varepsilon}}\boldsymbol{E} + \bar{\chi}_{eh}\boldsymbol{H}, \tag{1a}$$

$$\boldsymbol{B} = \bar{\boldsymbol{\mu}}\boldsymbol{H} + \bar{\chi}_{he}\boldsymbol{E}, \tag{1b}$$

where $\boldsymbol{D}/\boldsymbol{B}$ is the electric displacement vector/magnetic induction intensity, and $\boldsymbol{E}/\boldsymbol{H}$ is the electric/magnetic field. $\bar{\boldsymbol{\varepsilon}} = \varepsilon_0\bar{\boldsymbol{\varepsilon}}_r/\bar{\boldsymbol{\mu}} = \mu_0\bar{\boldsymbol{\mu}}_r$ is the permittivity/permeability tensor of the waveguide material. $\bar{\boldsymbol{\chi}}_{eh} = \sqrt{\varepsilon_0\mu_0}\bar{\boldsymbol{\chi}}^r_{eh}$ and $\bar{\boldsymbol{\chi}}_{he} = \sqrt{\varepsilon_0\mu_0}\bar{\boldsymbol{\chi}}^r_{he}$ are coupling constants. The material tensors are explicitly written as $\bar{\boldsymbol{\varepsilon}}_r = \begin{pmatrix} \bar{\boldsymbol{\varepsilon}}^{tt}_r & \bar{\boldsymbol{\varepsilon}}^{tz}_r \\ \bar{\boldsymbol{\varepsilon}}^{zt}_r & \bar{\boldsymbol{\varepsilon}}^{z}_r \end{pmatrix} = \begin{pmatrix} \varepsilon^{xx}_r & \varepsilon^{xy}_r & \varepsilon^{xz}_r \\ \varepsilon^{yx}_r & \varepsilon^{yy}_r & \varepsilon^{yz}_r \\ \varepsilon^{zx}_r & \varepsilon^{zy}_r & \varepsilon^{zz}_r \end{pmatrix}$, $\bar{\boldsymbol{\mu}}_r = \begin{pmatrix} \bar{\boldsymbol{\mu}}^{tt}_r & \bar{\boldsymbol{\mu}}^{tz}_r \\ \bar{\boldsymbol{\mu}}^{zt}_r & \bar{\boldsymbol{\mu}}^{z}_r \end{pmatrix} = \begin{pmatrix} \mu^{xx}_r & \mu^{xy}_r & \mu^{xz}_r \\ \mu^{yx}_r & \mu^{yy}_r & \mu^{yz}_r \\ \mu^{zx}_r & \mu^{zy}_r & \mu^{zz}_r \end{pmatrix}$, and $\bar{\boldsymbol{\chi}}^r_{he} = -\left[\bar{\boldsymbol{\chi}}^r_{eh}\right]^T = i\bar{\boldsymbol{\chi}} = i\begin{pmatrix} \chi_{xx} & \chi_{xy} & 0 \\ \chi_{yx} & \chi_{yy} & 0 \\ 0 & 0 & 0 \end{pmatrix}$. Here we concentrate on monochromatic electromagnetic waves with harmonic time dependency $e^{i\omega t}$. The electric and magnetic fields in waveguides obey the source-free Maxwell's equations: $\nabla\times\boldsymbol{E} = -i\omega\boldsymbol{B}, \nabla\times\boldsymbol{H} = i\omega\boldsymbol{D}$. Using normalized fields $\boldsymbol{e} = \boldsymbol{E}$ and $\boldsymbol{h} = \sqrt{\frac{\mu_0}{\varepsilon_0}}\boldsymbol{H}$ as well as the constitutive relation Eq. (1), the above Maxwell's equations are reformulated as,

$$\left[\nabla\times +ik_0\bar{\boldsymbol{\chi}}^r_{he}\right]\boldsymbol{e}_{3d}(x,y,z) + ik_0\bar{\boldsymbol{\mu}}_r\boldsymbol{h}_{3d}(x,y,z) = 0, \tag{2a}$$

$$\left[\nabla\times -ik_0\bar{\boldsymbol{\chi}}^r_{eh}\right]\boldsymbol{h}_{3d}(x,y,z) - ik_0\bar{\boldsymbol{\varepsilon}}_r\boldsymbol{e}_{3d}(x,y,z) = 0, \tag{2b}$$

where $k_0 = \omega\sqrt{\varepsilon_0\mu_0}$ is the vacuum wave number. Rewrite Eq. (2) in the following matrix form,

$$\begin{pmatrix} \nabla\times +ik_0\bar{\boldsymbol{\chi}}^r_{he} & ik_0\bar{\boldsymbol{\mu}}_r \\ -ik_0\bar{\boldsymbol{\varepsilon}}_r & \nabla\times -ik_0\bar{\boldsymbol{\chi}}^r_{eh} \end{pmatrix}\begin{pmatrix} \boldsymbol{e}_{3d}(x,y,z) \\ \boldsymbol{h}_{3d}(x,y,z) \end{pmatrix} = 0. \tag{3}$$

Considering the translational symmetry along the z axis, the position variables z and (x,y) in electric and magnetic fields can be separated,

$$\boldsymbol{e}_{3d}(x,y,z) = \boldsymbol{e}_{2d}(x,y)\,e^{-i\beta z} = \begin{pmatrix} e_x \\ e_y \\ e_z \end{pmatrix} e^{-i\beta z}, \tag{4a}$$

$$\boldsymbol{h}_{3d}(x,y,z) = \boldsymbol{h}_{2d}(x,y)\,e^{-i\beta z} = \begin{pmatrix} h_x \\ h_y \\ h_z \end{pmatrix} e^{-i\beta z}, \tag{4b}$$

where β is the propagation constant of mode $\boldsymbol{\phi}$. The reduced electromagnetic fields $\boldsymbol{e}_{2d}(x,y)$ and $\boldsymbol{h}_{2d}(x,y)$ only depend on the transverse coordinate (x,y). The effect of coordinate z is embodied in the exponential term $e^{-i\beta z}$.

Optics EXPRESS

Using the matrix form of differential operator in Cartesian coordinate system $\nabla\times = \begin{pmatrix} 0 & -\partial_z & \partial_y \\ \partial_z & 0 & -\partial_x \\ -\partial_y & \partial_x & 0 \end{pmatrix}$ and the relation $\partial_z = -i\beta$ when ∂_z acts on the fields in Eq. (4), we can further reformulate Eq. (3) into a six-component generalized eigen equation,

$$M\boldsymbol{\phi} = \beta N\boldsymbol{\phi}, \tag{5}$$

where the waveguide Hamiltonian M and the constant sigular matrix N are given by,

$$M = \begin{pmatrix} ik_0\chi_{xx} & ik_0\chi_{xy} & -i\partial_y & k_0\mu_r^{xx} & k_0\mu_r^{xy} & k_0\mu_r^{xz} \\ ik_0\chi_{yx} & ik_0\chi_{yy} & i\partial_x & k_0\mu_r^{yx} & k_0\mu_r^{yy} & k_0\mu_r^{yz} \\ i\partial_y & -i\partial_x & 0 & k_0\mu_r^{zx} & k_0\mu_r^{zy} & k_0\mu_r^{zz} \\ -k_0\varepsilon_r^{xx} & -k_0\varepsilon_r^{xy} & -k_0\varepsilon_r^{xz} & ik_0\chi_{xx} & ik_0\chi_{yx} & -i\partial_y \\ -k_0\varepsilon_r^{yx} & -k_0\varepsilon_r^{yy} & -k_0\varepsilon_r^{yz} & ik_0\chi_{xy} & ik_0\chi_{yy} & i\partial_x \\ -k_0\varepsilon_r^{zx} & -k_0\varepsilon_r^{zy} & -k_0\varepsilon_r^{zz} & i\partial_y & -i\partial_x & 0 \end{pmatrix}, \tag{6a}$$

$$N = \begin{pmatrix} 0 & -1 & 0 & 0 & 0 & 0 \\ 1 & 0 & 0 & 0 & 0 & 0 \\ 0 & 0 & 0 & 0 & 0 & 0 \\ 0 & 0 & 0 & 0 & -1 & 0 \\ 0 & 0 & 0 & 1 & 0 & 0 \\ 0 & 0 & 0 & 0 & 0 & 0 \end{pmatrix}. \tag{6b}$$

The eigenmode $\boldsymbol{\phi} = \boldsymbol{\phi}(x, y) = \left[e_x(x, y), e_y(x, y), e_z(x, y), h_x(x, y), h_y(x, y), h_z(x, y)\right]^T$. The superscript T denotes transpose operation. The propagation constant β is the generalized eigenvalue of (M, N) with eigenmode $\boldsymbol{\phi}$. It is observed that the Hamiltonian M defined in Eq. (6) contains only first order partial derivatives of x and y, which simplifies the calculations in the analysis of mode symmetry.

The eigen equation Eq. (5) determines a complete set of eigenmodes. We concentrate on the truncated mode set which contains eigenmodes labeled by the same quantum number. For waveguides that satisfy particular constraints, there are pairs of eigenmodes which degenerate in specified ways determined by the waveguide symmetry. One eigenmode can be transformed into its degenerate mode under the corresponding symmetry operation. The two eigenmodes in a degenerate mode pair can either propagate in opposite directions or in the same direction, but with different polarizations, depending on the commutation relation between the operator and Hamiltonian M as well as the matrix N. In the following subsections, we analyze several available symmetries and symmetry operations, as well as the material constraints ensuring each symmetry in detail.

2.2. Chiral operation and symmetry

At the beginning of our analysis, we introduce the chiral operation described by the unitary chiral operator σ,

$$\sigma = \begin{pmatrix} 1 & 0 & 0 & 0 & 0 & 0 \\ 0 & 1 & 0 & 0 & 0 & 0 \\ 0 & 0 & -1 & 0 & 0 & 0 \\ 0 & 0 & 0 & -1 & 0 & 0 \\ 0 & 0 & 0 & 0 & -1 & 0 \\ 0 & 0 & 0 & 0 & 0 & 1 \end{pmatrix}. \tag{7}$$

When the operator σ acts on eigenmode $\boldsymbol{\phi}$, it produces a new mode $\sigma\boldsymbol{\phi}$. It can be verified that the chiral operation keeps the x and y component of Poynting vector of the original mode $\boldsymbol{\phi}$ unchanged but reverses the z component. It indicates that the power flow direction of mode $\sigma\boldsymbol{\phi}$ is opposite to the direction of mode $\boldsymbol{\phi}$. Accordingly, chiral operator σ maps forward propagation modes to backward propagation modes. This property enables the chiral operation to establish degeneracy between two modes with opposite propagation directions. When the terms $\bar{\boldsymbol{\varepsilon}}_r^{zt}$, $\bar{\boldsymbol{\varepsilon}}_r^{tz}$, $\bar{\boldsymbol{\mu}}_r^{zt}$, $\bar{\boldsymbol{\mu}}_r^{tz}$ and $\bar{\boldsymbol{\chi}}$ equal to zero, the waveguide Hamiltonian M reduces to,

$$M = \begin{pmatrix} 0 & 0 & -i\partial_y & k_0\mu_r^{xx} & k_0\mu_r^{xy} & 0 \\ 0 & 0 & i\partial_x & k_0\mu_r^{yx} & k_0\mu_r^{yy} & 0 \\ i\partial_y & -i\partial_x & 0 & 0 & 0 & k_0\mu_r^{zz} \\ -k_0\varepsilon_r^{xx} & -k_0\varepsilon_r^{xy} & 0 & 0 & 0 & -i\partial_y \\ -k_0\varepsilon_r^{yx} & -k_0\varepsilon_r^{yy} & 0 & 0 & 0 & i\partial_x \\ 0 & 0 & -k_0\varepsilon_r^{zz} & i\partial_y & -i\partial_x & 0 \end{pmatrix}. \tag{8}$$

To discover the connection between the original mode $\boldsymbol{\phi}$ and the new mode $\sigma\boldsymbol{\phi}$, the commutation relation between operator σ and Hamiltonian M or the matrix N should be checked. Through matrix manipulation, one can find that chiral operator σ anticommutes with the reduced Hamiltonian M while commutes with the matrix N,

$$\sigma M \sigma^{-1} = -M, \tag{9a}$$

$$\sigma N \sigma^{-1} = N. \tag{9b}$$

Together with the eigen equation of the original mode $\boldsymbol{\phi}$, we have the following eigen equation for the new mode $\sigma\boldsymbol{\phi}$,

$$M\sigma\boldsymbol{\phi} = -\beta N \sigma\boldsymbol{\phi}. \tag{10}$$

Equation (10) implies if $\boldsymbol{\phi}$ is an eigenmode of (M, N) with eigenvalue β, then $\sigma\boldsymbol{\phi}$ is also an eigenmode with eigenvalue $-\beta$. The two degenerate modes propagate in opposite directions, and they are related by the chiral operation. In this case, the waveguide system maintains chiral symmetry, which requires the terms $\bar{\boldsymbol{\varepsilon}}_r^{zt}$, $\bar{\boldsymbol{\varepsilon}}_r^{tz}$, $\bar{\boldsymbol{\mu}}_r^{zt}$, $\bar{\boldsymbol{\mu}}_r^{tz}$ and $\bar{\boldsymbol{\chi}}$ to vanish. Notice that chiral symmetry defined here is different from the exact meaning of 'chiral' in the terminology of chiral media. Under our definition of chiral symmetry, the coupling constants are required to be zero, which physically means the forward and backward mode degeneracy specified by chiral symmetry can only be realized in media without bianisotropy, regardless of whether the media is chiral media or not.

Optics EXPRESS

2.3. Time reversal operation and symmetry

Next we continue to study the time reversal symmetry, which is described by the time reversal operator $\mathcal{T}$. Different from most of the operators appearing throughout this paper, the operator $\mathcal{T}$ is anti-unitary, which can be formally written as [18],

$$\mathcal{T} = UK, \tag{11}$$

where U is a unitary operator and K is the complex conjugate operator. As the operator K acts on a matrix, it takes complex conjugate of all the matrix elements. The effect when the operator $\mathcal{T}$ acts on mode $\boldsymbol{\phi}$ is $\mathcal{T}\boldsymbol{\phi} = UK\boldsymbol{\phi} = U\boldsymbol{\phi}^*$. The asterisk * denotes the complex conjugate operation. We take the operator U in the following matrix form,

$$U = \begin{pmatrix} 1 & 0 & 0 & 0 & 0 & 0 \\ 0 & 1 & 0 & 0 & 0 & 0 \\ 0 & 0 & 1 & 0 & 0 & 0 \\ 0 & 0 & 0 & -1 & 0 & 0 \\ 0 & 0 & 0 & 0 & -1 & 0 \\ 0 & 0 & 0 & 0 & 0 & -1 \end{pmatrix}. \tag{12}$$

The operator U defined in Eq. (12) reverses the sign of the magnetic field when it acts on an eigenmode. Similar to the chiral operator σ, the operator U also enables transformation between forward and backward propagation modes. If we impose the constraints that the matrix elements of $\bar{\boldsymbol{\varepsilon}}_r$, $\bar{\boldsymbol{\mu}}_r$ and $\bar{\boldsymbol{\chi}}$ are all real numbers, one shall obtain the following commutation relations,

$$\mathcal{T}M\mathcal{T}^{-1} = UM^*U^{-1} = -M, \tag{13a}$$

$$\mathcal{T}N\mathcal{T}^{-1} = N. \tag{13b}$$

Under the constraints, the time reversal operator $\mathcal{T}$ anticommutes with Hamiltonian M but commutes with the matrix N. Similar to the procedure of chiral symmetry, Eq. (13) leads to the following eigen equation,

$$M\mathcal{T}\boldsymbol{\phi} = -\beta^*N\mathcal{T}\boldsymbol{\phi}. \tag{14}$$

Consequently, providing $\boldsymbol{\phi}$ is the eigenmode of (M, N) with eigenvalue β, then $\mathcal{T}\boldsymbol{\phi}$ is also an eigenmode with eigenvalue $-\beta^*$. The propagation direction of one eigenmode is opposite to that of its degenerated mode due to the reversed sign of the propagation constant. Slightly different from chiral symmetry, the eigenvalue β not only reverses sign but also takes complex conjugate because of the anti-unitary property of the operator $\mathcal{T}$. Since the permittivity, permeability and coupling constants are real numbers, there is no gain or loss in the waveguide system. In this situation, the time reversal symmetry is preserved.

2.4. Parity operation and symmetry

The next symmetry operation we focus on is the parity operation, which is also a discrete operation like chiral and time reversal. The parity operation leads to space inversion. The coordinates (x, y) are denoted by the transverse position vector $\boldsymbol{r}$. Equation (15) gives that the parity operator $\mathcal{P}$ acts on mode $\boldsymbol{\phi}(\boldsymbol{r})$,

$$\mathcal{P}\boldsymbol{\phi}(\boldsymbol{r}) = Up\boldsymbol{\phi}(\boldsymbol{r}) = U\boldsymbol{\phi}(-\boldsymbol{r}), \tag{15}$$

where U is a unitary operator and p is the operator that reverses $\boldsymbol{r} \to -\boldsymbol{r}$. We take the matrix form of the operator U as defined in Eq. (12). Since the parity operator changes the transverse position

Optics EXPRESS

vector $\boldsymbol{r}$, we assume the material tensors to have spatial dependency, i.e. $\bar{\boldsymbol{\varepsilon}}_r(\boldsymbol{r})$, $\bar{\boldsymbol{\mu}}_r(\boldsymbol{r})$ and $\bar{\chi}(\boldsymbol{r})$. Then the coordinate dependency of the eigen equation Eq. (5) can be written explicitly as follows,

$$M(\partial_{\boldsymbol{r}}, \bar{\boldsymbol{\varepsilon}}_r(\boldsymbol{r}), \bar{\boldsymbol{\mu}}_r(\boldsymbol{r}), \bar{\chi}(\boldsymbol{r}))\boldsymbol{\phi}(\boldsymbol{r}) = \beta N \boldsymbol{\phi}(\boldsymbol{r}). \tag{16}$$

The notation $\partial_{\boldsymbol{r}}$ in Hamiltonian M denotes the position variables to be differentiated, which naturally fulfills $\partial_{-\boldsymbol{r}} = -\partial_{\boldsymbol{r}}$. All the rest $\boldsymbol{r}$s in Eq. (16) describes the spatial dependency of the material tensors and the wave function. If the spatial parameter distribution of waveguide fulfills $\bar{\boldsymbol{\varepsilon}}_r(\boldsymbol{r}) = \bar{\boldsymbol{\varepsilon}}_r(-\boldsymbol{r})$, $\bar{\boldsymbol{\mu}}_r(\boldsymbol{r}) = \bar{\boldsymbol{\mu}}_r(-\boldsymbol{r})$ and $\bar{\chi}(\boldsymbol{r}) = -\bar{\chi}(-\boldsymbol{r})$ under space inversion, we have the following commutation relations,

$$\mathcal{P}M\mathcal{P}^{-1} = UM(-\boldsymbol{r})U^{-1} = -M(\boldsymbol{r}), \tag{17a}$$

$$\mathcal{P}N\mathcal{P}^{-1} = N. \tag{17b}$$

As it is shown in Eq. (17), the operator $\mathcal{P}$ anticommutes with Hamiltonian M but commutes with the matrix N. Together with Eq. (5), the following eigen equation is obtained,

$$M\mathcal{P}\boldsymbol{\phi}(\boldsymbol{r}) = -\beta N\mathcal{P}\boldsymbol{\phi}(\boldsymbol{r}). \tag{18}$$

Therefore, $\mathcal{P}\boldsymbol{\phi}(\boldsymbol{r}) = U\boldsymbol{\phi}(-\boldsymbol{r})$ is an eigenmode of (M, N) with eigenvalue $-\beta$ provided $\boldsymbol{\phi}(\boldsymbol{r})$ is an eigenmode with eigenvalue β. Under the parity operation, a forward propagation mode is transformed to its degenerated backward propagation mode. Because of the space inversion effect, the degenerated forward and backward modes have different field distribution on the cross-section of waveguide. In this case, we regard the waveguide system to present parity symmetry.

2.5. $\mathcal{PT}$ operation and symmetry

We have examined the effects of parity symmetry and time reversal symmetry. The constraints to be fulfilled to guarantee each independent symmetry are derived. When combining the two symmetries together, it leads to $\mathcal{PT}$ (parity-time reversal) symmetry, which builds degeneracy between eigenmodes propagating in the same direcion. According to the combination of operations, the operator $\mathcal{PT}$ is direct product of the parity operator $\mathcal{P}$ and the time reversal operator $\mathcal{T}$. Because of the existence of the operator $\mathcal{T}$, the combined operator $\mathcal{PT}$ is also anti-unitary. When the opreator $\mathcal{PT}$ acts on mode $\boldsymbol{\phi}(\boldsymbol{r})$, it yields,

$$\mathcal{PT}\boldsymbol{\phi}(\boldsymbol{r}) = UpUK\boldsymbol{\phi}(\boldsymbol{r}) = UU\boldsymbol{\phi}^*(-\boldsymbol{r}) = \boldsymbol{\phi}^*(-\boldsymbol{r}). \tag{19}$$

Intuitively, the $\mathcal{PT}$ operation takes $\boldsymbol{r} \to -\boldsymbol{r}$ and complex conjugate of the wave function. If the waveguide material tensors fulfill the constraints that $\bar{\boldsymbol{\varepsilon}}_r(\boldsymbol{r}) = \bar{\boldsymbol{\varepsilon}}_r^*(-\boldsymbol{r})$, $\bar{\boldsymbol{\mu}}_r(\boldsymbol{r}) = \bar{\boldsymbol{\mu}}_r^*(-\boldsymbol{r})$ and $\bar{\chi}(\boldsymbol{r}) = -\bar{\chi}^*(-\boldsymbol{r})$, then we find the $\mathcal{PT}$ operator commutes with Hamiltonian M as well as the matrix N simultanously,

$$\mathcal{PT}M(\mathcal{PT})^{-1} = M^*(-\boldsymbol{r}) = M(\boldsymbol{r}), \tag{20a}$$

$$\mathcal{PT}N(\mathcal{PT})^{-1} = N. \tag{20b}$$

The commutation relation described in Eq. (20) results in the following eigen equation for the new mode $\mathcal{PT}\boldsymbol{\phi}$,

$$M\mathcal{PT}\boldsymbol{\phi} = \beta^* N\mathcal{PT}\boldsymbol{\phi}. \tag{21}$$

Equation (21) describes the degeneracy between two eigenmodes $\boldsymbol{\phi}(\boldsymbol{r})$ and $\boldsymbol{\phi}^*(-\boldsymbol{r})$, which are related by the $\mathcal{PT}$ operation and propagate in the same direction.

It is worth noting the phenomenon of $\mathcal{PT}$ symmetry broken and the related behaviour of eigenmodes and eigenvalues [11,19,20]. Before $\mathcal{PT}$ symmetry is broken, the propagation constant β is a real number, and the modes $\boldsymbol{\phi}(\boldsymbol{r})$ and $\boldsymbol{\phi}^*(-\boldsymbol{r})$ are the same eigenmode with eigenvalue β.

In other words, the eigenmodes are invariant under the $\mathcal{PT}$ operation. As the parameters of waveguide evolve beyond the exceptional point (EP), $\mathcal{PT}$ symmetry is spontaneously broken and the eigenvalue β turns to a complex number. In this case, the eigenvalues β and β^* form a conjugate pair. The degenerate modes $\boldsymbol{\phi}(\boldsymbol{r})$ and $\boldsymbol{\phi}^*(-\boldsymbol{r})$ become two different eigenmodes with the eigenvalue β and β^*, respectively. One eigenmode is transformed to its degenerated eigenmode under the $\mathcal{PT}$ operation.

2.6. Rotation operation and symmetry

In the previous subsections, we mainly discuss the degeneracy between forward and backward propagation eigenmodes (except $\mathcal{PT}$ symmetry). Here we proceed to study the degeneracy between two eigenmodes with the same propagation direction but different polarizations. There are mainly two opeations, namely rotation and mirror reflection, which are utilized to transform eigenmodes profiles. It is worth noting that eigenmode $\boldsymbol{\phi}(\boldsymbol{r})$ is the normalized electromagnetic field in waveguides, which is essentially a vector field. Rotating or mirror reflecting a vector field involves more than just coordinate transformation. To rotate a vector field $\boldsymbol{\phi}(\boldsymbol{r})$ by an angle θ about the z axis, we first rotate the coordinate $\boldsymbol{r}$ by θ to change the spatial position of the vector field while keeping the orientation of vectors unchanged. Then we rotate the field $\boldsymbol{\phi}(R^{-1}\boldsymbol{r})$ locally by θ without changing the spatial position of vectors. Accordingly, the rotation operator O_R acting on the eigenmode $\boldsymbol{\phi}(\boldsymbol{r})$ is defined as [15,16],

$$O_R\boldsymbol{\phi}(\boldsymbol{r}) = R_{ve}\boldsymbol{\phi}(R^{-1}\boldsymbol{r}), \tag{22}$$

where the vector rotation matrix $R_{ve}(\theta)$ and the coordinate rotation matrix $R(\theta)$ are given by,

$$R_{ve}(\theta) = \begin{pmatrix} \cos\theta & -\sin\theta & 0 & 0 & 0 & 0 \\ \sin\theta & \cos\theta & 0 & 0 & 0 & 0 \\ 0 & 0 & 1 & 0 & 0 & 0 \\ 0 & 0 & 0 & \cos\theta & -\sin\theta & 0 \\ 0 & 0 & 0 & \sin\theta & \cos\theta & 0 \\ 0 & 0 & 0 & 0 & 0 & 1 \end{pmatrix}, \tag{23a}$$

$$R(\theta) = \begin{pmatrix} \cos\theta & -\sin\theta \\ \sin\theta & \cos\theta \end{pmatrix}. \tag{23b}$$

The 6×6 matrix R_{ve} is for local rotation of the vector fields and the orthogonal matrix $R(\theta)$ is for coordinate rotation in two-dimensional space. If the material tensors of the waveguide fulfill the constraints that $R_{tz}\bar{\boldsymbol{\varepsilon}}_r\left(R^{-1}\boldsymbol{r}\right)R_{tz}{}^{-1} = \bar{\boldsymbol{\varepsilon}}_r(\boldsymbol{r})$, $R_{tz}\bar{\boldsymbol{\mu}}_r\left(R^{-1}\boldsymbol{r}\right)R_{tz}{}^{-1} = \bar{\boldsymbol{\mu}}_r(\boldsymbol{r})$ and $R_{tz}\bar{\chi}\left(R^{-1}\boldsymbol{r}\right)R_{tz}{}^{-1} = \bar{\chi}(\boldsymbol{r})$, where the matrix $R_{tz}(\theta) = \begin{pmatrix} R(\theta) & 0 \\ 0 & 1 \end{pmatrix}$, then one shall find the following commutation relations for the operator O_R,

$$O_R M O_R{}^{-1} = R_{ve}M(R^{-1}\boldsymbol{r})R_{ve}{}^{-1} = M(\boldsymbol{r}), \tag{24a}$$

$$O_R N O_R{}^{-1} = N. \tag{24b}$$

As a result, the operator O_R commutes with Hamiltonian M and the singular matrix N simultanously. Together with Eq. (5), the eigen equation for the new mode $O_R\boldsymbol{\phi}(\boldsymbol{r})$ is derived,

$$MO_R\boldsymbol{\phi}(\boldsymbol{r}) = \beta N O_R\boldsymbol{\phi}(\boldsymbol{r}). \tag{25}$$

Optics EXPRESS

As a result, provided $\boldsymbol{\phi}(\boldsymbol{r})$ is an eigenmode with eigenvalue β, then the rotated mode $O_R\boldsymbol{\phi}(\boldsymbol{r})$ is also an eigenmode with exactly the same eigenvalue. The eigenmode $O_R\boldsymbol{\phi}(\boldsymbol{r})$ can be the same as the eigenmode $\boldsymbol{\phi}(\boldsymbol{r})$, which means the mode $\boldsymbol{\phi}(\boldsymbol{r})$ is invariant under the rotation operation. Otherwise they are two eigenmodes with different polarizations, forming a degenerated mode pair. Taking the circular optical fiber as example, the TE/TM modes are unchanged under arbitrary rotation while the even and odd HE (EH) modes are transformed to each other by the rotation of certain angle θ. This difference bewteen TE/TM and HE/EH modes can be explained in theory and verified by the numerical simulation [16]. Note that the constraints to ensure rotation symmetry are more general than the intuitive rotational invariant waveguide.

2.7. Mirror reflection operation and symmetry

In analogy to rotation operation, the mirror reflection operation on vector field profiles also consists of two steps: (1) mirror reflection of the coordinate $\boldsymbol{r}$ to change the spatial position of the vector field without changing the orientation of vectors, (2) local mirror reflection of vectors with respect to the reflection axis while keeping the spatial position of vector field. Assume the reflection axis goes through the origin at an angle θ with the x axis. The formal expression of the mirror reflection operator O_S acting on mode $\boldsymbol{\phi}(\boldsymbol{r})$ is written as follows,

$$O_S\boldsymbol{\phi}(\boldsymbol{r}) = S_{ve}\boldsymbol{\phi}(S^{-1}\boldsymbol{r}), \tag{26}$$

where the vector mirror reflection matrix $S_{ve}(\theta)$ and the coordinate mirror reflection matrix $S(\theta)$ are given by,

$$S_{ve}(\theta) = \begin{pmatrix} \cos 2\theta & \sin 2\theta & 0 & 0 & 0 & 0 \\ \sin 2\theta & -\cos 2\theta & 0 & 0 & 0 & 0 \\ 0 & 0 & 1 & 0 & 0 & 0 \\ 0 & 0 & 0 & -\cos 2\theta & -\sin 2\theta & 0 \\ 0 & 0 & 0 & -\sin 2\theta & \cos 2\theta & 0 \\ 0 & 0 & 0 & 0 & 0 & -1 \end{pmatrix}, \tag{27a}$$

$$S(\theta) = \begin{pmatrix} \cos 2\theta & \sin 2\theta \\ \sin 2\theta & -\cos 2\theta \end{pmatrix}. \tag{27b}$$

The matrix S_{ve} is for local mirror reflection, and it has another function. Since the usual mirror reflection changes the chiral property of electromagnetic field, the propagation direction of the symmetric mode is opposite to the original mode. However, here we aim to build degeneracy between eigenmodes propagating in the same direction but with different polarizations. Hence we define the operator S_{ve} to reverse the direction of magnetic field in order to keep the propagation direction unchanged under the mirror reflection operation. When the waveguide system fulfills the constraints that $S_{tz}\bar{\boldsymbol{\varepsilon}}_r\left(S^{-1}\boldsymbol{r}\right)S_{tz}{}^{-1} = \bar{\boldsymbol{\varepsilon}}_r\left(\boldsymbol{r}\right)$, $S_{tz}\bar{\boldsymbol{\mu}}_r\left(S^{-1}\boldsymbol{r}\right)S_{tz}{}^{-1} = \bar{\boldsymbol{\mu}}_r\left(\boldsymbol{r}\right)$ and $S_{tz}\bar{\boldsymbol{\chi}}\left(S^{-1}\boldsymbol{r}\right)S_{tz}{}^{-1} = -\bar{\boldsymbol{\chi}}\left(\boldsymbol{r}\right)$, where $S_{tz}\left(\theta\right) = \begin{pmatrix} S\left(\theta\right) & 0 \\ 0 & 1 \end{pmatrix}$, then we have the following commutation relations for the operator O_S,

$$O_S M O_S{}^{-1} = S_{ve}M(S^{-1}\boldsymbol{r})S_{ve}{}^{-1} = -M(\boldsymbol{r}), \tag{28a}$$

$$O_S N O_S{}^{-1} = -N. \tag{28b}$$

The operator O_S anticommutes with Hamiltonian M and the matrix N simultanously. Using this commutation relation, the eigen equation for the new mode $O_S\boldsymbol{\phi}(\boldsymbol{r})$ is derived,

$$MO_S\boldsymbol{\phi}(\boldsymbol{r}) = \beta NO_S\boldsymbol{\phi}(\boldsymbol{r}). \tag{29}$$

Therefore, if $\boldsymbol{\phi}(\boldsymbol{r})$ is an eigenmode of (M, N) with eigenvalue β, then the image mode $O_S\boldsymbol{\phi}(\boldsymbol{r})$ is a degenerated eigenmode with the same eigenvalue as well.

2.8. Combination of symmetries

Having analyzed six elementary symmetries in detail, we list the conclusions in Table 1. In this section, we are in a position to discuss the combination of symmetry operations. The combined symmetry operation can lead to new symmetry under some constraints without requiring each individual symmetry to hold. To demonstrate this, take the combination of parity and time reversal symmetry as well as the $\mathcal{PT}$ symmetry as example. The material tensors are required to satisfy $\bar{\boldsymbol{\varepsilon}}_r(\boldsymbol{r}) = \bar{\boldsymbol{\varepsilon}}_r^*(-\boldsymbol{r})$, $\bar{\boldsymbol{\mu}}_r(\boldsymbol{r}) = \bar{\boldsymbol{\mu}}_r^*(-\boldsymbol{r})$ and $\bar{\chi}(\boldsymbol{r}) = -\bar{\chi}^*(-\boldsymbol{r})$ to guarantee $\mathcal{PT}$ symmetry. However, this constraint does not guarantee the independent parity symmetry and time reversal symmetry at the same time. Conversely, if the waveguide system possesses the two symmetries simultaneously, then it holds $\mathcal{PT}$ symmetry as well.

Table 1. Symmetry and degeneracy of waveguide modes

	Commutation relation	Degeneracy	Constraints
Chiral symmetry	$\sigma M\sigma^{-1} = -M$ $\sigma N\sigma^{-1} = N$	$\boldsymbol{\psi}_{-\beta} = \sigma\boldsymbol{\phi}_\beta$	$\bar{\boldsymbol{\varepsilon}}_r^{zt} = \bar{\boldsymbol{\varepsilon}}_r^{tz} = 0$ $\bar{\boldsymbol{\mu}}_r^{zt} = \bar{\boldsymbol{\mu}}_r^{tz} = 0$ $\bar{\chi} = 0$
Time reversal symmetry	$\mathcal{T}M\mathcal{T}^{-1} = -M$ $\mathcal{T}N\mathcal{T}^{-1} = N$	$\boldsymbol{\psi}_{-\beta^*} = \mathcal{T}\boldsymbol{\phi}_\beta = U\boldsymbol{\phi}_\beta^*$	$\bar{\boldsymbol{\varepsilon}}_r = \bar{\boldsymbol{\varepsilon}}_r^*$ $\bar{\boldsymbol{\mu}}_r = \bar{\boldsymbol{\mu}}_r^*$ $\bar{\chi} = \bar{\chi}^*$
Parity symmetry	$\mathcal{P}M\mathcal{P}^{-1} = -M$ $\mathcal{P}N\mathcal{P}^{-1} = N$	$\boldsymbol{\psi}_{-\beta}(\boldsymbol{r}) = \mathcal{P}\boldsymbol{\phi}_\beta(\boldsymbol{r})$ $= U\boldsymbol{\phi}_\beta(-\boldsymbol{r})$	$\bar{\boldsymbol{\varepsilon}}_r(\boldsymbol{r}) = \bar{\boldsymbol{\varepsilon}}_r(-\boldsymbol{r})$ $\bar{\boldsymbol{\mu}}_r(\boldsymbol{r}) = \bar{\boldsymbol{\mu}}_r(-\boldsymbol{r})$ $\bar{\chi}(\boldsymbol{r}) = -\bar{\chi}(-\boldsymbol{r})$
$\mathcal{PT}$ symmetry	$\mathcal{PT}M(\mathcal{PT})^{-1} = M$ $\mathcal{PT}N(\mathcal{PT})^{-1} = N$	$\boldsymbol{\psi}_{\beta^*}(\boldsymbol{r}) = \mathcal{PT}\boldsymbol{\phi}_\beta(\boldsymbol{r})$ $= \boldsymbol{\phi}_\beta^*(-\boldsymbol{r})$	$\bar{\boldsymbol{\varepsilon}}_r(\boldsymbol{r}) = \bar{\boldsymbol{\varepsilon}}_r^*(-\boldsymbol{r})$ $\bar{\boldsymbol{\mu}}_r(\boldsymbol{r}) = \bar{\boldsymbol{\mu}}_r^*(-\boldsymbol{r})$ $\bar{\chi}(\boldsymbol{r}) = -\bar{\chi}^*(-\boldsymbol{r})$
Rotation symmetry	$O_RMO_R^{-1} = M$ $O_RNO_R^{-1} = N$	$\boldsymbol{\psi}_\beta(\boldsymbol{r}) = O_R\boldsymbol{\phi}_\beta(\boldsymbol{r})$ $= R_{ve}\boldsymbol{\phi}_\beta(R^{-1}\boldsymbol{r})$	$R_{tz}\bar{\boldsymbol{\varepsilon}}_r\left(R^{-1}\boldsymbol{r}\right)R_{tz}^{-1} = \bar{\boldsymbol{\varepsilon}}_r(\boldsymbol{r})$ $R_{tz}\bar{\boldsymbol{\mu}}_r\left(R^{-1}\boldsymbol{r}\right)R_{tz}^{-1} = \bar{\boldsymbol{\mu}}_r(\boldsymbol{r})$ $R_{tz}\bar{\chi}\left(R^{-1}\boldsymbol{r}\right)R_{tz}^{-1} = \bar{\chi}(\boldsymbol{r})$
Mirror reflection symmetry	$O_SMO_S^{-1} = -M$ $O_SNO_S^{-1} = -N$	$\boldsymbol{\psi}_\beta(\boldsymbol{r}) = O_S\boldsymbol{\phi}_\beta(\boldsymbol{r})$ $= S_{ve}\boldsymbol{\phi}_\beta(S^{-1}\boldsymbol{r})$	$S_{tz}\bar{\boldsymbol{\varepsilon}}_r\left(S^{-1}\boldsymbol{r}\right)S_{tz}^{-1} = \bar{\boldsymbol{\varepsilon}}_r(\boldsymbol{r})$ $S_{tz}\bar{\boldsymbol{\mu}}_r\left(S^{-1}\boldsymbol{r}\right)S_{tz}^{-1} = \bar{\boldsymbol{\mu}}_r(\boldsymbol{r})$ $S_{tz}\bar{\chi}\left(S^{-1}\boldsymbol{r}\right)S_{tz}^{-1} = -\bar{\chi}(\boldsymbol{r})$

Despite this, if we assume the two individual symmetries to be hold, then the constraints of the combined symmetry can be derived from elementary symmetries conveniently. For instance, the parity and rotation operation can be combined together to get a new symmetry operation $\mathcal{P}O_R$. When the operator $\mathcal{P}O_R$ acts on mode $\boldsymbol{\phi}(\boldsymbol{r})$, it leads to,

$$\mathcal{P}O_R\boldsymbol{\phi}(\boldsymbol{r}) = UR_{ve}\boldsymbol{\phi}(-R^{-1}\boldsymbol{r}). \tag{30}$$

Since we assume parity and rotation symmetry, then the commutation relations of these two symmetry hold, from which we get the following relations,

$$\mathcal{P}O_R M(\mathcal{P}O_R)^{-1} = -M, \tag{31a}$$

$$\mathcal{P}O_R N(\mathcal{P}O_R)^{-1} = N. \tag{31b}$$

Equation (31) indicates that the parity-rotation symmetry produces degenerate mode pairs propagating in opposite directions. The constraints that ensure this new symmetry come from the combination of the constraints for parity and rotation symmetry. Taking the permittivity tensor as example,

$$\bar{\boldsymbol{\varepsilon}}_r(\boldsymbol{r}) = \bar{\boldsymbol{\varepsilon}}_r(-\boldsymbol{r}), R_{tz}\bar{\boldsymbol{\varepsilon}}_r\left(R^{-1}\boldsymbol{r}\right)R_{tz}{}^{-1} = \bar{\boldsymbol{\varepsilon}}_r(\boldsymbol{r}), \tag{32a}$$

$$\to R_{tz}\bar{\boldsymbol{\varepsilon}}_r\left(R^{-1}\boldsymbol{r}\right)R_{tz}{}^{-1} = \bar{\boldsymbol{\varepsilon}}_r(-\boldsymbol{r}). \tag{32b}$$

Similarly, the constraints for the permeability and coupling constants are $R_{tz}\bar{\boldsymbol{\mu}}_r\left(R^{-1}\boldsymbol{r}\right)R_{tz}{}^{-1} = \bar{\boldsymbol{\mu}}_r(-\boldsymbol{r})$ and $R_{tz}\bar{\chi}\left(R^{-1}\boldsymbol{r}\right)R_{tz}^{-1} = -\bar{\chi}(-\boldsymbol{r})$, respectively.

3. Results and discussions

In this section, we revisit several waveguides with different properties such as balanced gain and loss, anisotropy, and geometrical symmetry. The operating wavelength in all simulations is set to $\lambda_0 = 1\mu m$. The eigenmodes and propagation constants are calculated by full-wave simulation using COMSOL Multiphysics [21].

3.1. $\mathcal{PT}$ symmetry in waveguides with balanced gain and loss

To illustrate $\mathcal{PT}$ symmetry clearly, we consider the $\mathcal{PT}$ symmetric waveguide system with balanced gain and loss as discussed in [22]. As shown in the inset of Fig. 1, the structure consists of two waveguides with the same geometric dimensions placed close to each other. The width of the rectangular cross-section of waveguides is $0.3\mu m$ and the height is $0.2\mu m$. The separation between two waveguides is set to $0.03\mu m$. The two waveguides are isotropic and surrounded by the background air. The permittivity is $\varepsilon_r = 10 - i\Delta\varepsilon$ for the left core and $\varepsilon_r = 10 + i\Delta\varepsilon$ for the right core. Obviously, the material tensor fulfills the constraints for $\mathcal{PT}$ symmetry that $\bar{\boldsymbol{\varepsilon}}_r(\boldsymbol{r}) = \bar{\boldsymbol{\varepsilon}}_r^*(-\boldsymbol{r})$. It is known that a pair of even and odd super modes is formed in this structure. The effective mode index $n_{eff} = \beta/k_0$, then the behaviour of n_{eff} is equivalent to the eigenvalue β. As revealed in Fig. 1, as the parameter $\Delta\varepsilon$ increases from zero, the real parts of two eigenvalues become close to each other while the imaginary parts remain to be zero. The $\mathcal{PT}$ symmetry is spontaneously broken when $\Delta\varepsilon$ reaches the exceptional point and evolve beyond it. In this situation, the real parts of two eigenvalues merge together, while the imaginary parts bifurcate. The exceptional point of this structure is between $\Delta\varepsilon = 0.2$ and 0.3. Before the $\mathcal{PT}$ symmetry is broken ($\Delta\varepsilon = 0.05$), the eigenvalues are $n_{eff} = 2.1705$ and 2.2671. The eigenmodes are invariant under the parity operation ($\boldsymbol{r} \to -\boldsymbol{r}$) and time reversal operation (complex conjugate). After the $\mathcal{PT}$ symmetry is broken ($\Delta\varepsilon = 0.3$), the eigenvalues are $n_{eff} = 2.2189 \pm 0.021538i$. The two eigenmodes become a degenerated mode pair and tranform to each other under the $\mathcal{PT}$ operation. Therefore the behaviours of eigenvalues and eigenmodes before and after $\mathcal{PT}$ symmetry broken are consistent with the predictions from Section 2.5.

3.2. Chiral, time reversal, and parity symmetry in general anisotropic waveguides

In order to demonstrate the characteristics of chiral, time reversal, and parity symmetry visually, we study the eigenmodes of four anisotropic waveguides, each of which is constructed to possess some symmetry. The geometric structures of waveguides A, B, C and D are shown in row 1,2,3 and 4 of Fig. 2, respectively. All waveguide cross-sections are 0.5 μm wide and 0.3 μm high. The

Optics EXPRESS

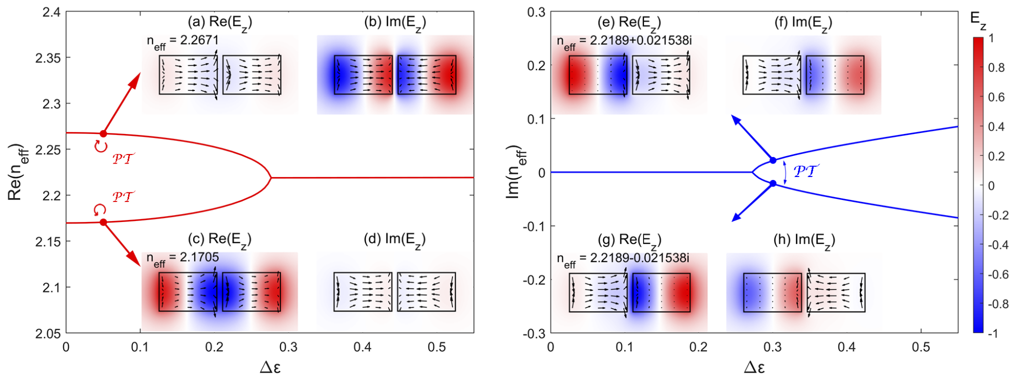

Fig. 1. The evolution of real and imaginary part of effective mode indices n_{eff} with respect to $\Delta\varepsilon$. The insets show the electric field of two modes at $\Delta\varepsilon = 0.05$ (inset (a/b) and (c/d)) and $\Delta\varepsilon = 0.3$ (inset (e/f) and (g/h)). The vector plots represent the x and y components, and the color plots represent the z components. All fields have been under global phase adjustment and normalized to the range of -1 to 1.

cross-sections of waveguides A and B are rectangles with one angle removed, therefore parity symmetry is broken in the two structures. The cross-sections of waveguides C and D are elliptic and rectangular, respectively. Therefore, they both preserve parity symmetry. The permittivity tensors of the four waveguides are listed in Table 2. According to the constraints of elementary symmetries, chiral symmetry is satisfied in waveguide A, but time reversal symmetry is broken by the complex terms in $\bar{\boldsymbol{\varepsilon}}_r^A$. Waveguide B possesses time reversal symmetry but breaks chiral symmetry. Waveguide C breaks both chiral and time reversal symmetry, which can be inferred from $\bar{\boldsymbol{\varepsilon}}_r^C$. As a comparison of the three examples above, waveguide D satisfies both chiral and time reversal symmetry.

Table 2. Three symmetry operations on the eigenmodes of four different type of waveguides A, B, C and D. A/B/C only has chiral/time reversal/parity symmetry, while D has all the three types of symmetry. The symbol ✓indicates that the new mode obtained by the operation is still an eigenmode, while the symbol × indicates that the new mode is no longer an eigenmode.

	Chiral operation	Time reversal operation	Parity operation	Permittivity tensor
A	✓	×	×	$\bar{\boldsymbol{\varepsilon}}_r^A = \begin{pmatrix} 8 & 3i & 0 \\ -3i & 8 & 0 \\ 0 & 0 & 8 \end{pmatrix}$
B	×	✓	×	$\bar{\boldsymbol{\varepsilon}}_r^B = \begin{pmatrix} 8 & 0 & 3 \\ 0 & 8 & 0 \\ 3 & 0 & 8 \end{pmatrix}$
C	×	×	✓	$\bar{\boldsymbol{\varepsilon}}_r^C = \begin{pmatrix} 10 & 0 & 4i \\ 0 & 10 & 0 \\ -4i & 0 & 10 \end{pmatrix}$
D	✓	✓	✓	$\bar{\boldsymbol{\varepsilon}}_r^D = \begin{pmatrix} 8 & 3 & 0 \\ 3 & 8 & 0 \\ 0 & 0 & 8 \end{pmatrix}$

For electric fields, the chiral operation is to invert the z component, the time reversal operation is to take complex conjugate of the field, and the parity operation causes space inversion ($\boldsymbol{r} \longrightarrow -\boldsymbol{r}$).

Optics EXPRESS

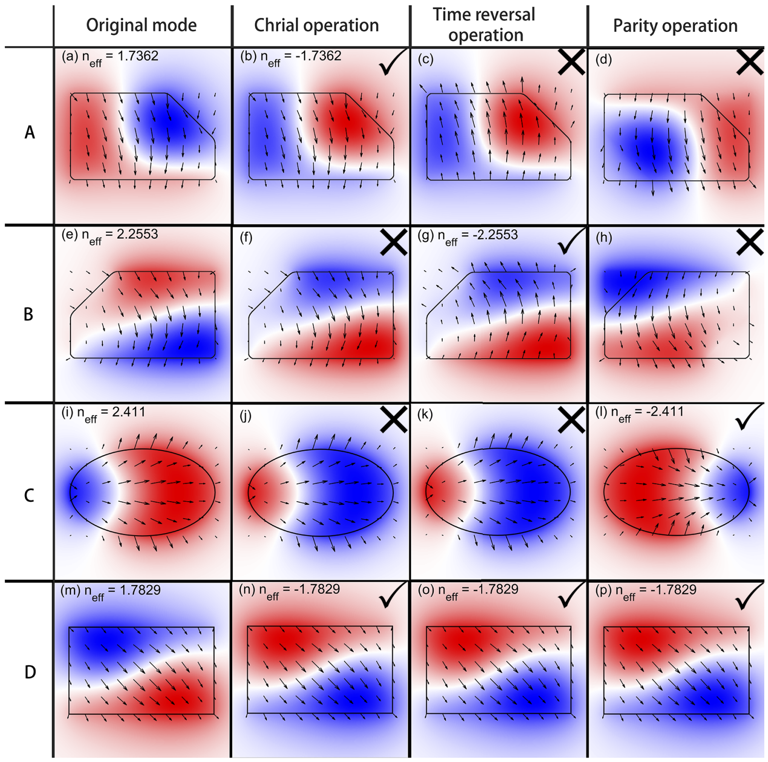

Fig. 2. Normalized electric fields before and after symmetry operations in waveguide A,B,C and D. The arrow plots show the x and y components of electric fields, and the color plots show z components. Subplots (a) to (h) show the imaginary part of x, y and z field components. Electric fields in subplots (i) to (p) have been under global phase adjustment, so that x and y components are real and z components are pure imaginary.

The behaviours of eigenmodes of each waveguide under the three symmetry operations are listed in Table 2, which are consistent with the previous predictions. As shown in Fig. 2, the first column depicts the original eigenmodes of waveguide A,B,C and D from top to bottom. The second, third and fourth columns show the new fields obtained by chiral, time reversal and parity operation, respectively. The symbols ✓and ✕ in Fig. 2 show which subplot represents a legitimate eigenmode and which plot does not.

The chiral, time reversal and parity operation establish symmetry relations between forward and backward propagation modes, which are shown in Fig. 3. From top to bottom, the three mode profiles on the left are forward eigenmodes of waveguides A,B and C respectively. The profiles of the backward degenerate modes obtained by the three operations are depicted on the right. Since the chiral and time reversal operation do not involve coordinate transformation, the transverse coordinates (x, y) of points A_1 and A_2 on the reference plane are the same as point A in Fig. 3. The parity operation causes space inversion, therefore point A_3 and A are symmetric with respect to the origin.

In coupled mode theory, the new eigenmodes of the waveguide after perturbation are expanded by the forward and backward propagation modes of the unperturbed waveguide. When applying CMT in waveguides with one of the three symmetries above, one can take advantage of the corresponding symmetry operation to derive backward modes from forward modes conveniently. Then, the forward and backward modes form a complete mode set [11].

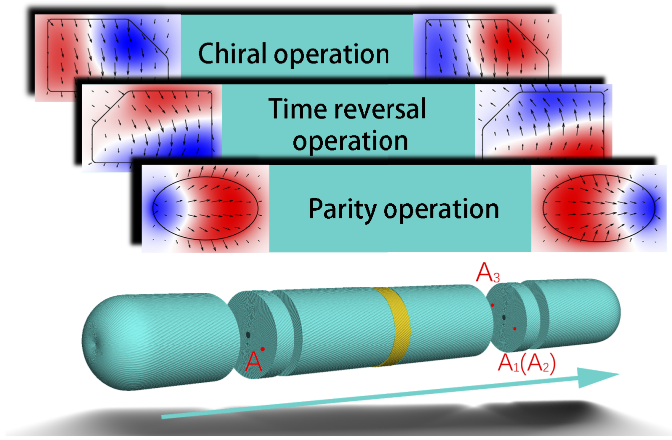

Fig. 3. The symmetry relations between forward and backward propagation modes. Point A is on the reference plane of the forward propagation mode, and A_1, A_2 and A_3 are corresponding points on the reference plane of the backward propagation mode obtained under chiral, time reversal and parity operations, respectively. The yellow plane in the middle is the mirror plane between the forward and backward direction.

4. Conclusion

In summary, we propose a simple yet effective approach to study the waveguide mode symmetry by reformulating the waveguide problem into generalized eigenvalue problems determined by the matrices (M, N), which turns out that the mode symmetry is purely determined by M. Thereby, the analysis of M is sufficient and necessary condition for analysing the waveguide mode symmetry, and is much easier than previous 4×4 Hamiltonian approach containing second-order partial derivatives. With this approach, we analyze six common symmetries in waveguides, of which three symmetries (chiral, time reversal, parity) establish degeneracy between forward and backward propagation modes, and the other three symmetries ($\mathcal{PT}$, rotation, mirror reflection) establish degeneracy between modes propagating in the same direction. In Section 3, we analyze the behaviour of eigenvalues and eigenmodes before and after $\mathcal{PT}$ symmetry broken in detail. We also compare the differences of chiral, time reversal and parity symmetry in anisotropic waveguides.

Generally, our framework can be applied to the symmetry analysis of any waveguide system. The categories of symmetry are not limited to those mentioned in this research, but may also be categories that have not been studied previously. Once the symmetry operators are correctly defined in this framework, commutation relations for the new symmetry can be derived according to similar procedures discussed earlier. Thus, our method opens the way to studying new symmetries that have rarely been examined before, and even the hidden symmetries in optics [23]. Without exactly solving Maxwell's equations, our approach can be used to analyze the properties of optical systems directly, which can be useful for the analysis and design of waveguide structures or other photonic circuits.

Funding. National Key Research and Development Program of China (2021YFB2800303); Innovation Project of Optics Valley Laboratory; National Natural Science Foundation of China (61405067).

Disclosures. The authors declare no conflicts of interest.

Data availability. Data underlying the results presented in this paper are not publicly available at this time but may be obtained from the authors upon reasonable request.

Optics EXPRESS

References

1. J. Schwichtenberg, *Physics from Symmetry* (Springer International Publishing AG, 2018).
2. K. Sakoda, *Optical Properties of Photonic crystals* (Springer-Verlag, 2005).
3. W. Chen, Q. Yang, Y. Chen, and W. Liu, "Scattering activities bounded by reciprocity and parity conservation," Phys. Rev. Res. **2**(1), 013277 (2020).
4. W. Chen, Q. Yang, Y. Chen, and W. Liu, "Global Mie Scattering: Polarization Morphologies and the Underlying Topological Invariant," ACS Omega **5**(23), 14157–14163 (2020).
5. C. M. Bender and S. Boettcher, "Real Spectra in Non-Hermitian Hamiltonians Having $\mathcal{PT}$ Symmetry," Phys. Rev. Lett. **80**(24), 5243–5246 (1998).
6. C. Rüter, K. Makris, R. El-Ganainy, D. Christodoulides, M. Segev, and D. Kip, "Observation of parity–time symmetry in optics," Nat. Phys. **6**(3), 192–195 (2010).
7. K. Makris, R. El-Ganainy, D. Christodoulides, and Z. Musslimani, "Beam Dynamics in $\mathcal{PT}$ Symmetric Optical Lattices," Phys. Rev. Lett. **100**(10), 103904 (2008).
8. K. Makris, R. El-Ganainy, D. Christodoulides, and Z. Musslimani, "$\mathcal{PT}$-symmetric optical lattices," Phys. Rev. A **81**(6), 063807 (2010).
9. J. W. Yoon, Y. Choi, C. Hahn, G. Kim, S. H. Song, K. Yang, J. Y. Lee, Y. Kim, C. S. Lee, J. K. Shin, H. Lee, and P. Berini, "Time-asymmetric loop around an exceptional point over the full optical communications band," Nature **562**(7725), 86–90 (2018).
10. Y. Zhang, W. Liu, H. Long, K. Wang, B. Wang, and P. Lu, "Chiral/directional mode transfer based on a tunable non-Hermitian system," Opt. Express **29**(26), 44146–44156 (2021).
11. J. Xu and Y. Chen, "General coupled mode theory in non-Hermitian waveguides," Opt. Express **23**(17), 22619–22627 (2015).
12. W. Chen, Z. Xiong, J. Xu, and Y. Chen, "Generalized coupled-mode formalism in reciprocal waveguides with gain, loss, anisotropy, or bianisotropy," Phys. Rev. B **99**(19), 195307 (2019).
13. L. Fang, H. Wang, Y. Liang, H. Cao, and J. Wang, "Spin-Orbit Mapping of Light," Phys. Rev. Lett. **127**(23), 233901 (2021).
14. J. Wang, S. Chen, and J. Liu, "Orbital angular momentum communications based on standard multi-mode fiber," APL Photonics **6**(6), 060804 (2021).
15. J. D. Joannopoulos, S. G. Johnson, J. N. Winn, and R. D. Meade, *Photonic crystals: molding the flow of light* (Princeton University Press, 2008).
16. Z. Xiong, W. Chen, P. Wang, and Y. Chen, "Classification of symmetry properties of waveguide modes in presence of gain/losses, anisotropy/bianisotropy, or continuous/discrete rotational symmetry," Opt. Express **25**(24), 29822–29834 (2017).
17. M. Skorobogatiy, S. Jacobs, S. Johnson, and Y. Fink, "Geometric variations in high index-contrast waveguides, coupled mode theory in curvilinear coordinates," Opt. Express **10**(21), 1227–1243 (2002).
18. J. J. Sakurai, *Modern Quantum Mechanics* (Addison-Wesley Publishing Company, 1994).
19. C. M. Bender, S. Boettcher, and P. N. Meisinger, "$\mathcal{PT}$-symmetric quantum mechanics," J. Math. Phys. **40**(5), 2201–2229 (1999).
20. A. Guo, G. Salamo, D. Duchesne, R. Morandotti, M. Volatier-Ravat, V. Aimez, G. Siviloglou, and D. Christodoulides, "Observation of $\mathcal{PT}$-Symmetry Breaking in Complex Optical Potentials," Phys. Rev. Lett. **103**(9), 093902 (2009).
21. COMSOL Multiphysics 5.6: a finite element analysis, solver and simulation software. http://www.comsol.com/.
22. S. Klaiman, U. Günther, and N. Moiseyev, "Visualization of Branch Points in $\mathcal{PT}$-Symmetric Waveguides," Phys. Rev. Lett. **101**(8), 080402 (2008).
23. Z. Xiong, R. Zhang, R. Yu, C. T. Chan, and Y. Chen, "Hidden-symmetry-enforced nexus points of nodal lines in layer-stacked dielectric photonic crystals," Light: Sci. Appl. **9**(1), 176 (2020).